Acta Crystallographica Section C
Crystal Structure Communications
ISSN 0108-2701

Two polymorphs and the diethylammonium salt of the barbiturate eldoral

Thomas Gelbrich,* Denise Rossi and Ulrich J. Griesser

Institute of Pharmacy, University of Innsbruck, Innrain 52c, 6020 Innsbruck, Austria
Correspondence e-mail: thomas.gelbrich@uibk.ac.at

Received 25 October 2011
Accepted 21 December 2011
Online 6 January 2012

Polymorph (I*a*) of eldoral [5-ethyl-5-(piperidin-1-yl)barbituric acid or 5-ethyl-5-(piperidin-1-yl)-1,3-diazinane-2,4,6-trione], $C_{11}H_{17}N_3O_3$, displays a hydrogen-bonded layer structure parallel to (100). The piperidine N atom and the barbiturate carbonyl group in the 2-position are utilized in N—H···N and N—H···O=C hydrogen bonds, respectively. The structure of polymorph (I*b*) contains pseudosymmetry elements. The two independent molecules of (I*b*) are connected *via* N—H···O=C(4/6-position) and N—H···N(piperidine) hydrogen bonds to give a chain structure in the [100] direction. The hydrogen-bonded layers, parallel to (010), formed in the salt diethylammonium 5-ethyl-5-(piperidin-1-yl)barbiturate [or diethylammonium 5-ethyl-2,4,6-trioxo-5-(piperidin-1-yl)-1,3-diazinan-1-ide], $C_4H_{12}N^+\cdot C_{11}H_{16}N_3O_3^-$, (II), closely resemble the corresponding hydrogen-bonded structure in polymorph (I*a*). Like many other 5,5-disubstituted derivatives of barbituric acid, polymorphs (I*a*) and (I*b*) contain the $R_2^2(8)$ N—H···O=C hydrogen-bond motif. However, the overall hydrogen-bonded chain and layer structures of (I*a*) and (I*b*) are unique because of the involvement of the hydrogen-bond acceptor function in the piperidine group.

Comment

As part of a larger investigation of derivatives of barbituric acid (Gelbrich *et al.*, 2007, 2010*a*,*b*, 2011; Zencirci *et al.*, 2009, 2010; Gelbrich, Zencirci *et al.*, 2010), we have studied two solid forms of 5-ethyl-5-(piperidin-1-yl)barbituric acid, (I) (CAS No. 509-87-5), and its diethylammonium salt, (II). Compound (I), also known as eldoral, has been marketed as a sedative and hypnotic drug since 1936 (Anders, 1954). According to Brandstätter-Kuhnert & Aepkers (1962), three distinct polymorphs of (I) grow from the melt. Their melting points were given as 490 (form I), 483 (form II; also the polymorph of the sublimate investigated by Fischer, 1939) and 477 K (form III). From sublimation experiments at 473 K, we obtained polymorph (I*a*) as long needles and polymorph (I*b*) as blocks. Crystals of (I*a*) and (I*b*) also formed concomitantly from an ethanol solution. The results of thermomicroscopic and differential scanning calorimetry experiments confirmed (I*a*) and (I*b*) to be identical to forms I and II, respectively, studied by Brandstätter-Kuhnert & Aepkers (1962). The diethylammonium salt, (II), was obtained by slow evaporation of a solution of (I) in diethylamine.

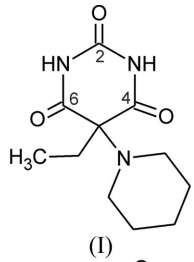

(I)

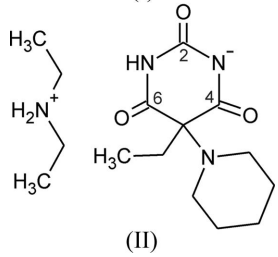

(II)

As expected, the barbiturate entity adopts the same principle geometry (Fig. 1) in all three investigated crystal structures. The barbiturate ring is essentially planar and the piperidine ring has a chair conformation. The ethyl conformation is such that the C2···C5—C7—C8 pseudo-torsion angle is close to 0°, and C8—C7—C5—N9 is close to 180° (see Table 4).

The relative geometry of the five potential hydrogen-bond donor or acceptor functions of a barbiturate ring (two NH and three carbonyl groups, respectively) is inflexible. As a result, certain standard N—H···O=C hydrogen-bonded structures are frequently observed in 5,5-substituted derivatives of barbituric acid, usually one of four common chain structures (Gelbrich *et al.*, 2011). In categorizing these structures, it is

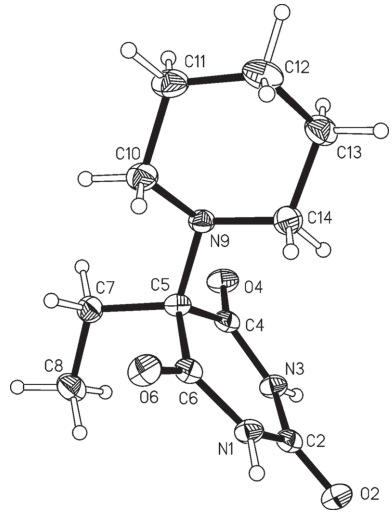

Figure 1
The asymmetric unit of (I*a*). Displacement ellipsoids are drawn at the 50% probability level.

 doi:10.1107/S0108270111055120

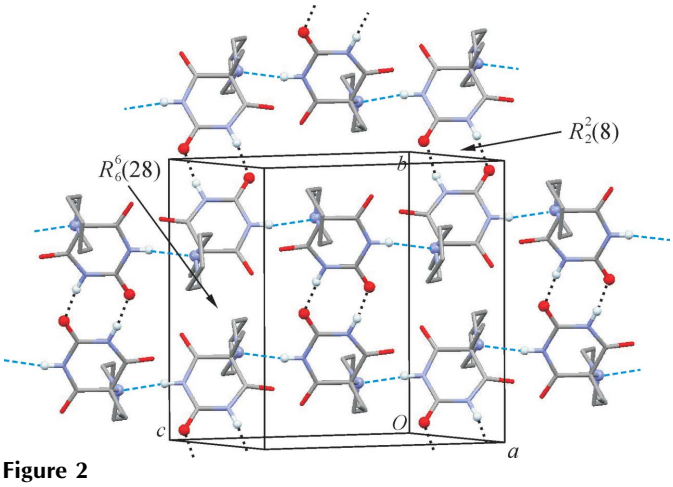

Figure 2
The hydrogen-bonded layer structure of (I*a*). H, O and N atoms directly involved in N—H···O (dotted lines) or N—H···N (dashed lines) interactions are drawn as balls.

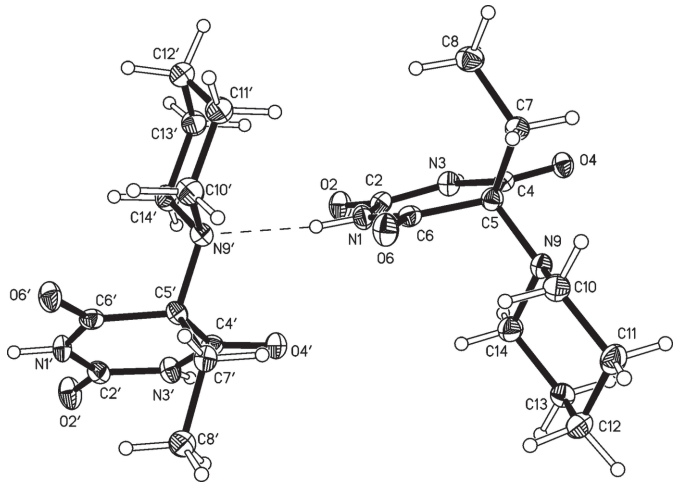

Figure 3
The asymmetric unit of (I*b*). Displacement ellipsoids are drawn at the 50% probability level. The primed molecule is molecule *B*.

useful to distinguish between the two topologically equivalent carbonyl groups in the 4- and 6-positions on the one hand and the carbonyl group in the 2-position on the other. In the case of eldoral, (I), the piperidine N atom can be utilized as an additional hydrogen-bond acceptor, which increases the number of feasible hydrogen-bond motifs.

The crystal structure of (I*a*) contains one independent molecule (Fig. 1). Two barbiturate rings are N—H···O=C hydrogen bonded to one another *via* a centrosymmetric $R_2^2(8)$ ring (Etter *et al.*, 1990), and this interaction involves the C2 carbonyl group. One N—H···N hydrogen bond links each barbiturate ring to the piperidine group of a second molecule that is related to the first by a *c*-glide operation. Overall, the N—H···O=C and N—H···N interactions (Table 1) result in a corrugated layer structure parallel to (100) with $p2_1/b$ layer symmetry. It contains larger $R_6^6(28)$ rings connecting four molecules (Fig. 2).

The asymmetric unit of the second polymorph, (I*b*), consists of two molecules (denoted *A* and *B*, Fig. 3). The barbiturate rings of *A*- and *B*-type molecules are doubly N—H···O=C hydrogen bonded to one another so that an $R_2^2(8)$ ring is formed (Table 2). In contrast with the situation found in (I*a*), one of the two equivalent C4/C6-carbonyl groups in each molecule is utilized in this interaction (rather than the C2 group). The resulting 'dimeric' N—H···O=C hydrogen-bonded unit is connected to two other units of the same kind *via* N—H···N(piperidine) interactions, so that *A*- and *B*-type molecules are linked to one another as a consequence. An infinite hydrogen-bonded chain structure parallel to [100] is generated (Fig. 4), which contains centrosymmetric $R_4^4(18)$ rings that link four molecules together.

The nature of single-component crystal structures containing more than one independent molecule ($Z' > 1$) has been discussed by several authors in recent years (Steiner, 2000; Steed, 2003; Desiraju, 2007; Anderson & Steed, 2007; Bernstein, 2011). In order to gain a better understanding of such a crystal structure, it is useful to establish the geometric differences and commonalities between its Z' independent molecular environments, and thereby the presence (or absence) of local or peudosymmetry elements in the crystal structure. For example, investigations with the computer program *XPac* (Gelbrich & Hursthouse, 2005) have revealed that local symmetry elements are present in a $Z' = 4$ form of carbamazepine (Gelbrich & Hursthouse, 2006), as well as in a $Z' = 2$ polymorph of sulfathiazole (Gelbrich *et al.*, 2008).

An analogous *XPac* analysis for the structure of (I*b*) reveals that its two complete molecular shells around *A* and *B* (each consisting of $n = 15$ molecules) exhibit roughly the same geometry, *i.e.* molecules *A* and *B* are related to one another by an approximate symmetry transformation. However, a relatively high *XPac* dissimilarity index *x* (Fabbiani *et al.*, 2009) of 9.9 (calculated for $n = 15$) for the two independent molecular shells of *A* and *B* is obtained, which indicates that the deviation from proper symmetry relationships is considerable.

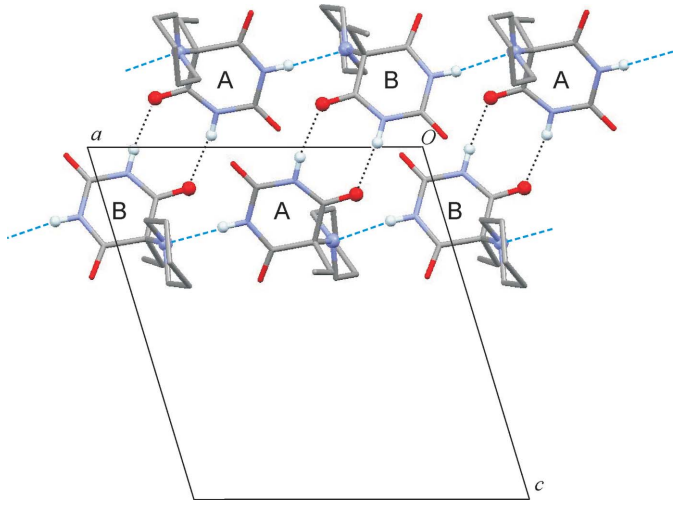

Figure 4
The hydrogen-bonded chain structure of (I*b*), viewed along [010]. H, O and N atoms directly involved in N—H···O (dotted lines) or N—H···N (dashed lines) interactions are drawn as balls.

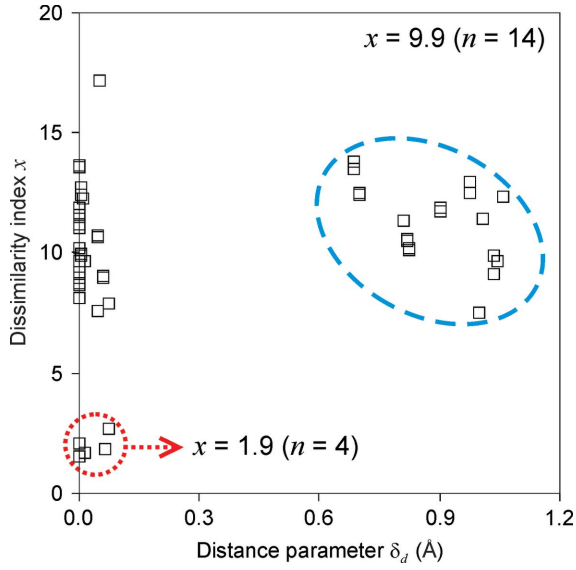

Figure 5
An *XPac* plot for the comparison of the geometrically similar shells of $n = 15$ molecules around molecules *A* and *B* of polymorph (I*b*). A subset of data points for $n = 5$ (encircled by a dotted line) lies close to the origin (implying a high degree of similarity). It represents the hydrogen-bonded chain shown in Fig. 4, which has a noncrystallographic glide symmetry. A second subset of data points (encircled by a dashed line) indicates relatively large differences in the distances.

More details can be deduced from the diagram in Fig. 5. For each comparison between a pair of molecules in shell *A* with the matching pair in shell *B*, the individual dissimilarity parameter x_i is plotted against the corresponding distance parameter $\delta_{d,i}$. The latter is the absolute difference of the distances between the two respective molecular centroids in the shells of *A* and *B*, and some of the differences are as high as 1 Å (data points encircled by a dashed line). However, a subset of data points (encircled by a dotted line) lies much closer to the origin than the rest, and it gives a combined *x* value of just 1.9 (for $n = 4$). These data points correspond to a shell fragment of five neighbouring molecules, which in turn represents the hydrogen-bonded chain shown in Fig. 4. Overall, the *XPac* results are consistent with an approximate *C*2/*c* pseudosymmetry of (I*b*), in which the pseudo-glide symmetry (perpendicular to [010]; glide vector parallel to [100]) between hydrogen-bonded *A* and *B* molecules is particularly well preserved.

Fig. 6 shows the asymmetric unit of the diethylammonium salt, (II). The NH group of the barbiturate ring is hydrogen bonded to the piperidine ring of the next molecule (Table 3). This interaction alone results in an extended chain parallel to [100] [translation of 11.8270 (3) Å], as the two molecules are related by an *a*-glide plane perpendicular to [001] (Fig. 7). An *XPac* comparison reveals that it has the same geometry as the corresponding N—H···N hydrogen-bonded chain propagating along [001] [translation of 11.9438 (3) Å] in polymorph (I*a*). The *XPac* dissimilarity index *x* for this one-dimensional supramolecular construct is 5.3 (for $n = 2$). The NH_2 group of the cation of (II) acts as a bridge between two anions, *i.e. via* an N—H···O=C hydrogen bond to the C2 carbonyl group of

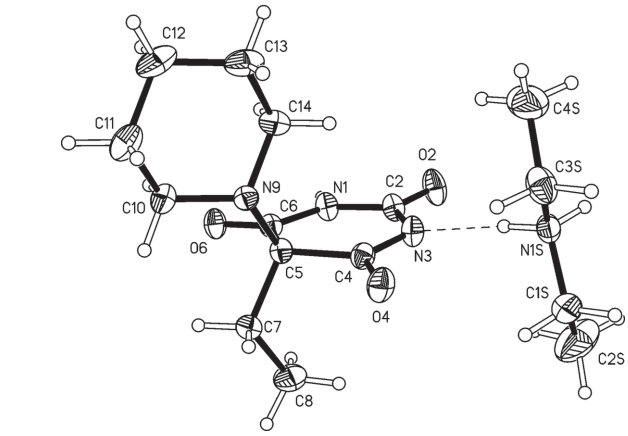

Figure 6
The asymmetric unit of (II). Displacement ellipsoids are drawn at the 50% probability level.

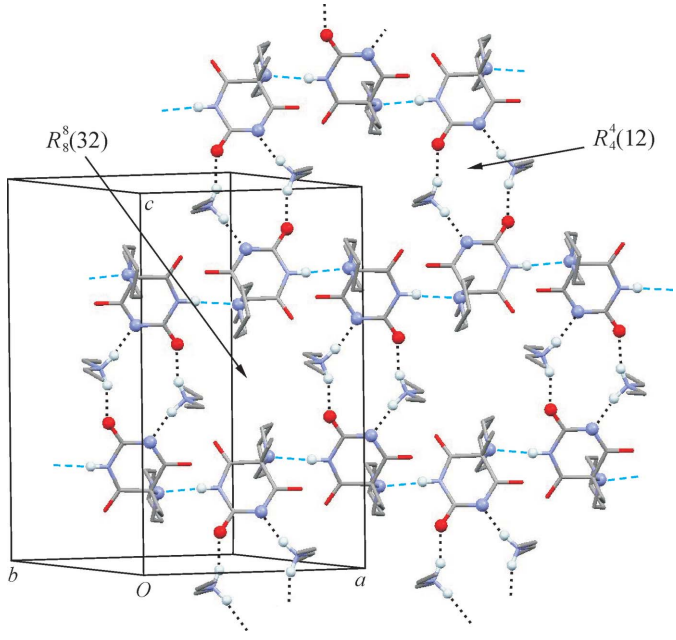

Figure 7
The two-dimensional hydrogen-bonded chain structure of (II). H, O and N atoms directly involved in O···H—N—H···O hydrogen bonds with the cation (dotted lines) or N—H···N(piperidine) interactions (dashed lines) are drawn as balls.

the first anion and *via* an N—H···N hydrogen bond to the N3 atom of the second anion. Neighbouring anions are thereby doubly-bridged so that a centrosymmetric $R_4^4(12)$ ring is formed. This interaction, in combination with the anion–anion N—H···N hydrogen bonds, results in a hydrogen-bonded layer which lies parallel to (001).

In Fig. 8, the hydrogen-bonded structures of (I*a*), (I*b*) and (II) are compared with those of two analogous 5,5-substituted barbituric acid derivatives with N—H···*A* hydrogen bonds (*A* = hydrogen-bond acceptor), *viz.* 3-oxocyclobarbital [Cambridge Structural Database (Allen, 2002) refcode BARCOX; Chentli-Benchikha *et al.*, 1977] and bromo-*meso*-sarcosinuric acid (BMBARA10; Pascard-Billy, 1970). The barbiturate ring is represented as a hexagon, with N—H groups drawn as

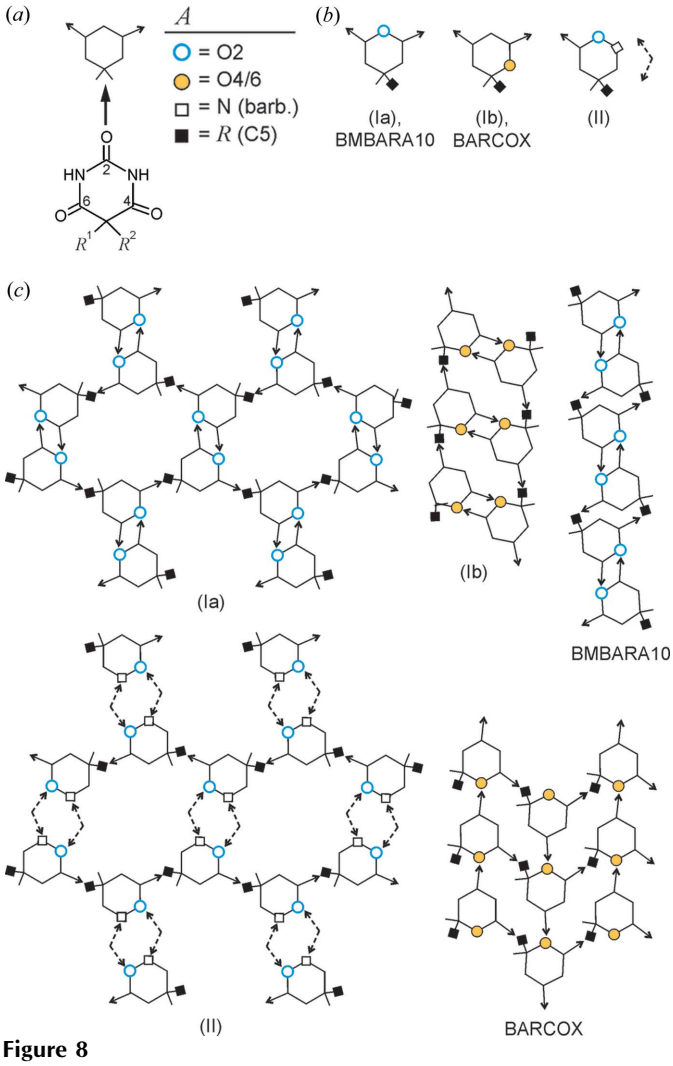

Figure 8
A comparison of the hydrogen-bonded structures of 5,5-disubsituted derivatives of barbituric acid with a single utilized hydrogen-bond acceptor function in a 5-substituted group. (*a*) Simplified representation of a barbiturate molecule, with N—H donor groups drawn as arrows and different types of hydrogen-bond acceptor (*A*) functions as either circles or squares. (*b*) The configuration of the utilized hydrogen-bond donor and acceptor functions in each molecule. (*c*) One-dimensional [(I*b*) and BMBARA10] and two-dimensional [(I*a*), (II) and BARCOX] extended hydrogen-bonded structures. Note the similarity between (I*a*) and (II).

arrows and the utilized hydrogen-bond acceptor sites as either circles (barbiturate carbonyl group), filled squares (5-substituted group, *R*) or open squares (deprotonated barbiturate N atom) (Figs. 8*a* and 8*b*). The close one-dimensional relationship between the hydrogen-bonded structures of (I*a*) and (II) discussed above is apparent from Fig. 8(*c*). Moreover, the N—H···O=C $R_2^2(8)$ linkage between adjacent N—H···N(piperidine) hydrogen-bonded chains in (I*a*) is neatly substituted in (II) for two mutually opposite N···H—N—H···O bridges *via* a central cation. This similarity between (I*a*) and (II) may also indicate a feasible transition mechanism for the removal of diethylamine from (II). Indeed, phase identification on the basis of FT–IR spectra has indicated that, upon solvent loss, the crystals of (II) transform exclusively into form (I*a*).

For each structure, the configuration of utilized hydrogen-bond donor and acceptor sites is illustrated in Fig. 8(*b*). Polymorph (I*a*) has the same configuration as BMBARA10, while (I*b*) exhibits the same characteristics as BARCOX. However, quite different one- and two-dimensional hydrogen-bonded structures result from this within each of the two pairs. We note that there are only two recurring hydrogen-bonded motifs within this set. One is the $C(5)$ chain motif found in (I*a*) and (II), and the other is the $R_2^2(8)$ ring motif involving the *A* function of the C2 carbonyl group, which is present in (I*a*) and in BMBARA10.

Experimental

The sample of eldoral, (I), used in this study had been stored in our laboratory for almost 50 years. The reports of Aepkers (1961) and Brandstätter-Kuhnert & Aepkers (1962) imply a commercially available product as its origin, without giving further details. Suitable crystals of (I*a*) and (I*b*) were obtained from an ethanol solution. Crystals of (II) were obtained in an NMR tube by evaporation of a dilute solution of (I) in diethylamine. The FT–IR spectra of (I*a*) and (I*b*) are available in the *Supplementary materials*. All *XPac* (Gelbrich & Hursthouse, 2005) calculations cited in the *Comment* were carried out with a complete set of 17 non-H atomic positions of the barbiturate molecule.

Polymorph (I*a*)

Crystal data

$C_{11}H_{17}N_3O_3$
M_r = 239.28
Monoclinic, $P2_1/c$
a = 7.8761 (2) Å
b = 12.7102 (4) Å
c = 11.9438 (3) Å
β = 98.189 (3)°
V = 1183.46 (6) Å^3
Z = 4
Cu $K\alpha$ radiation
μ = 0.82 mm^{-1}
T = 173 K
0.43 × 0.40 × 0.40 mm

Data collection

Oxford Xcalibur Ruby Gemini Ultra diffractometer
Absorption correction: multi-scan (*CrysAlis PRO*; Oxford Diffraction, 2003)
T_{min} = 0.719, T_{max} = 0.735
6405 measured reflections
2111 independent reflections
1900 reflections with $I > 2\sigma(I)$
R_{int} = 0.030

Refinement

$R[F^2 > 2\sigma(F^2)]$ = 0.044
$wR(F^2)$ = 0.126
S = 1.09
2117 reflections
178 parameters
2 restraints
H atoms treated by a mixture of independent and constrained refinement
$\Delta\rho_{max}$ = 0.21 e Å^{-3}
$\Delta\rho_{min}$ = −0.21 e Å^{-3}

Polymorph (I*b*)

Crystal data

$C_{11}H_{17}N_3O_3$
M_r = 239.28
Monoclinic, $P2_1/n$
a = 11.9311 (3) Å
b = 15.9858 (4) Å
c = 13.0768 (3) Å
β = 106.799 (1)°
V = 2387.68 (10) Å^3
Z = 8
Mo $K\alpha$ radiation
μ = 0.10 mm^{-1}
T = 120 K
0.25 × 0.04 × 0.04 mm

Table 1
Hydrogen-bond geometry (Å, °) for polymorph (I*a*).

D—H···A	D—H	H···A	D···A	D—H···A
N1—H1···N9^{i}	0.86 (1)	2.13 (2)	2.9843 (16)	172 (2)
N3—H3···O2^{ii}	0.88 (2)	1.97 (2)	2.8295 (16)	165 (2)

Symmetry codes: (i) $x, -y+\frac{1}{2}, z+\frac{1}{2}$; (ii) $-x+1, -y+1, -z+1$.

Table 2
Hydrogen-bond geometry (Å, °) for polymorph (I*b*).

D—H···A	D—H	H···A	D···A	D—H···A
N1—H1···N9′	0.89 (2)	2.13 (2)	3.012 (3)	173 (3)
N3—H3···O4′^{i}	0.88 (2)	2.05 (2)	2.901 (3)	161 (3)
N1′—H1′···N9^{ii}	0.89 (2)	2.19 (2)	3.072 (3)	168 (2)
N3′—H3′···O4^{i}	0.87 (2)	2.04 (2)	2.870 (3)	159 (3)

Symmetry codes: (i) $-x+1, -y, -z$; (ii) $x+1, y, z$.

Table 3
Hydrogen-bond geometry (Å, °) for (II).

D—H···A	D—H	H···A	D···A	D—H···A
N1—H1···N9^{i}	0.87 (1)	2.15 (1)	3.0136 (13)	174 (1)
N1*S*—H1*SA*···N3	0.93 (1)	1.84 (1)	2.7555 (13)	169 (1)
N1*S*—H1*SB*···O2^{ii}	0.90 (1)	1.86 (1)	2.7204 (13)	159 (1)

Symmetry codes: (i) $x-\frac{1}{2}, y, -z+\frac{1}{2}$; (ii) $-x+1, -y, -z$.

Data collection

Bruker–Nonius Kappa diffractometer with a Roper CCD camera, using a rotating anode system
Absorption correction: multi-scan (*SADABS*; Sheldrick, 2007)
T_{min} = 0.976, T_{max} = 0.996
20817 measured reflections
4211 independent reflections
3314 reflections with $I > 2\sigma(I)$
R_{int} = 0.074

Refinement

$R[F^2 > 2\sigma(F^2)]$ = 0.063
$wR(F^2)$ = 0.140
S = 1.05
4211 reflections
356 parameters
4 restraints
H atoms treated by a mixture of independent and constrained refinement
$\Delta\rho_{max}$ = 0.30 e Å^{-3}
$\Delta\rho_{min}$ = −0.25 e Å^{-3}

Compound (II)

Crystal data

$C_4H_{12}N^+\cdot C_{11}H_{16}N_3O_3^-$
M_r = 312.41
Orthorhombic, *Pbca*
a = 11.8270 (3) Å
b = 16.1719 (4) Å
c = 18.6774 (5) Å
V = 3572.35 (16) Å^3
Z = 8
Cu $K\alpha$ radiation
μ = 0.67 mm^{-1}
T = 173 K
0.20 × 0.15 × 0.15 mm

Data collection

Oxford Xcalibur Ruby Gemini Ultra diffractometer
Absorption correction: multi-scan (*CrysAlis PRO*; Oxford Diffraction, 2003)
T_{min} = 0.880, T_{max} = 1.000
25972 measured reflections
3209 independent reflections
2921 reflections with $I > 2\sigma(I)$
R_{int} = 0.034

Table 4
Torsion angles (°) in the barbiturate molecules (I*a*), (I*b*) and (II).

Structure	C2···C5—C7—C8	C8—N7—C5—N1
(I*a*)	−4.38 (16)	172.20 (11)
(I*b*), molecule *A*	0.5 (2)	176.2 (2)
(I*b*), molecule *B*†	−1.5 (3)	−177.5 (2)
(II)	2.70 (13)	−172.63 (9)

† C2′···C5′—C7′—C8′ and C8′—N7′—C5′—N1′

Refinement

$R[F^2 > 2\sigma(F^2)]$ = 0.035
$wR(F^2)$ = 0.097
S = 1.04
3209 reflections
240 parameters
3 restraints
H atoms treated by a mixture of independent and constrained refinement
$\Delta\rho_{max}$ = 0.34 e Å^{-3}
$\Delta\rho_{min}$ = −0.21 e Å^{-3}

All H atoms were identified in a difference Fourier map. Methyl H atoms were idealized (C—H = 0.98 Å) and included as rigid groups allowed to rotate but not to tip, while methylene H atoms were positioned geometrically (C—H = 0.99 Å) and refined using a riding model. H atoms on N atoms were refined with the N—H distances restrained to 0.88 (2) Å. The U_{iso} parameters of all H atoms were refined freely.

Data collection: *CrysAlis PRO* (Oxford Diffraction, 2003) for (I*a*) and (II); *COLLECT* (Nonius, 1998) for (I*b*). Cell refinement: *CrysAlis PRO* for (I*a*) and (II); *SCALEPACK* (Otwinowski & Minor, 1997) for (I*b*). Data reduction: *CrysAlis PRO* for (I*a*) and (II); *DENZO* (Otwinowski & Minor, 1997) and *SCALEPACK* for (I*b*). For all compounds, program(s) used to solve structure: *SHELXS97* (Sheldrick, 2008); program(s) used to refine structure: *SHELXL97* (Sheldrick, 2008); molecular graphics: *XP* in *SHELXTL* (Bruker, 1998) and *Mercury* (Macrae *et al.*, 2008); software used to prepare material for publication: *publCIF* (Westrip, 2010).

TG gratefully acknowledges financial support from the Lise Meitner Programme of the Austrian Science Fund (FWF, project No. M1135-N17). We thank Professor Volker Kahlenberg (Innsbruck) and Dr Simon Coles (Southampton) for access to the X-ray instruments used in this study.

Supplementary data for this paper are available from the IUCr electronic archives (Reference: SK3420). Services for accessing these data are described at the back of the journal.

References

Aepkers, M. (1961). Dissertation, University of Innsbruck, Austria.
Allen, F. H. (2002). *Acta Cryst.* B**58**, 380–388.
Anders, H. (1954). *Pharm. Zentralhalle Dtschl*, **93**, 5–7.
Anderson, K. M. & Steed, J. W. (2007). *CrystEngComm*, **9**, 328–330.
Bernstein, J. (2011). *Cryst. Growth Des.* **11**, 632–650.
Brandstätter-Kuhnert, M. & Aepkers, M. (1962). *Microchim. Acta*, **50**, 1055–1074.
Bruker (1998). *XP*. Bruker AXS Inc., Madison, Wisconsin, USA
Chentli-Benchikha, F., Declercq, J. P., Germain, G., Van Meerssche, M., Bouché, R. & Draguet-Brughmans, M. (1977). *Acta Cryst.* B**33**, 2739–2743.
Desiraju, G. R. (2007). *CrystEngComm*, **9**, 91–92.
Etter, M. C., MacDonald, J. C. & Bernstein, J. (1990). *Acta Cryst.* B**46**, 256–262.
Fabbiani, F. P. A., Dittrich, B., Florence, A. J., Gelbrich, T., Hursthouse, M. B., Kuhs, W. F., Shankland, N. & Sowa, H. (2009). *CrystEngComm*, **11**, 1396–1406.

Fischer, R. (1939). *Arch. Pharm.* **277**, 305–321.
Gelbrich, T., Hughes, D. S., Hursthouse, M. B. & Threlfall, T. L. (2008). *CrystEngComm*, **10**, 1328–1334.
Gelbrich, T. & Hursthouse, M. B. (2005). *CrystEngComm*, **7**, 324–336.
Gelbrich, T. & Hursthouse, M. B. (2006). *CrystEngComm*, **8**, 448–460.
Gelbrich, T., Rossi, D. & Griesser, U. J. (2010*a*). *Acta Cryst.* E**66**, o1219.
Gelbrich, T., Rossi, D. & Griesser, U. J. (2010*b*). *Acta Cryst.* E**66**, o2688.
Gelbrich, T., Rossi, D., Häfele, C. A. & Griesser, U. J. (2011). *CrystEngComm*, **13**, 5502–5509.
Gelbrich, T., Zencirci, N. & Griesser, U. J. (2007). *Acta Cryst.* C**63**, o751–o753.
Gelbrich, T., Zencirci, N. & Griesser, U. J. (2010). *Acta Cryst.* C**66**, o55–o58.
Macrae, C. F., Bruno, I. J., Chisholm, J. A., Edgington, P. R., McCabe, P., Pidcock, E., Rodriguez-Monge, L., Taylor, R., van de Streek, J. & Wood, P. A. (2008). *J. Appl. Cryst.* **41**, 466–470.
Nonius (1998). *COLLECT*. Nonius BV, Delft, The Netherlands.
Otwinowski, Z. & Minor, W. (1997). *Methods in Enzymology*, Vol. 276, *Macromolecular Crystallography*, Part A, edited by C. W. Carter Jr & R. M. Sweet, pp. 307–326. New York: Academic Press.
Oxford Diffraction (2003). *CrysAlis CCD* and *CrysAlis RED*. Oxford Diffraction Ltd, Abingdon, Oxfordshire, England.
Pascard-Billy, C. (1970). *Acta Cryst.* B**26**, 1418–1425.
Sheldrick, G. M. (2007). *SADABS*. University of Göttingen, Germany.
Sheldrick, G. M. (2008). *Acta Cryst.* A**64**, 112–122.
Steed, J. W. (2003). *CrystEngComm*, **5**, 169–179.
Steiner, T. (2000). *Acta Cryst.* B**56**, 673–676.
Westrip, S. P. (2010). *J. Appl. Cryst.* **43**, 920–925.
Zencirci, N., Gelbrich, T., Apperley, D. C., Harris, R. K., Kahlenberg, V. & Griesser, U. J. (2010). *Cryst. Growth Des.* **10**, 302–313.
Zencirci, N., Gelbrich, T., Kahlenberg, V. & Griesser, U. J. (2009). *Cryst. Growth Des.* **9**, 3444–3456.